High-throughput plasma proteomic platforms: Insights from a multi-ethnic Asian cohort

Authors:
Akash Bahai*[1], He Wang*[1], Pritesh R Jain[1], Lucas D Ward[2], Oleksandr Boychenko [3], Zhihao Ding [4], Jun Frederiksen [5], Joanne Ngeow[1,6], Jimmy Lee[1,7], Elio Riboli[1,8], Jianjun Liu[9], Sebastian Maurer-Stroh[10,11], Enrico Petretto[12,13], Ching-Yu Cheng[11,14,15], Bernett Lee[1], Saumya Shekhar Jamuar[16], Nicolas Bertin[9], Claire Bellis[9], Max Lam[1,17], Weiling Zheng[17], Xueling Sim[18], Patrick Tan[9,17,19,20], John C Chambers[#1,8,17], Nilanjana Sadhu[#1]

*equal contributions
[#]equal contributions

Affiliations:
[1]Lee Kong Chian School of Medicine, Nanyang Technological University, Singapore
[2]Alnylam Pharmaceuticals, Cambridge, MA, USA
[3]Bayer AG, Wuppertal, Germany
[4]Boehringer Ingelheim Pharma GmbH & Co. KG, Biberach, Germany
[5] Novo Nordisk A/S, Copenhagen, Denmark
[6]Cancer Genetics Service, National Cancer Centre, Singapore
[7]North Region, Institute of Mental Health, Singapore
[8]Department of Epidemiology and Biostatistics, Imperial College London, London, UK
[9]Genome Institute of Singapore, Agency for Science, Technology and Research (A∗STAR), Singapore
[10]Bioinformatics Institute, Agency for Science, Technology and Research (A∗STAR), Singapore
[11]Yong Loo Lin School of Medicine, National University of Singapore, Singapore
[12]Programme in Cardiovascular and Metabolic Disorders, Duke-NUS Medical School, Singapore
[13]Centre for Computational Biology, Duke-NUS Medical School, Singapore
[14]Singapore Eye Research Institute, Singapore National Eye Centre, Singapore
[15]Ophthalmology and Visual Sciences Academic Clinical Program (Eye ACP), Duke-NUS Medical School, Singapore
[16]KK Women's and Children's Hospital, Duke-NUS Institute of Precision Medicine, Singapore
[17]Precision Health Research, Singapore, Singapore
[18]Saw Swee Hock School of Public Health, National University of Singapore, Singapore
[19]SingHealth Duke-NUS Institute of Precision Medicine, Singapore
[20]Cancer & Stem Cell Biology Program, Duke-NUS Medical School, Singapore

Corresponding authors: John C Chambers (john.chambers@ntu.edu.sg), Nilanjana Sadhu (nilanjana.sadhu@ntu.edu.sg)

Abstract

We compared three leading affinity-based and mass-spectrometry-based proteomic platforms (SomaScan11K, Olink Explore HT, Orbitrap Astral with Seer Proteograph [MS-Seer]) in a multi-ethnic Asian cohort, to inform biomarker discovery and functional genomic studies of global populations. We found limited overlap (1,740 proteins) across the three platforms, with modest correlations (0.34-0.10). SomaScan had lower missingness (<1%) and CV (<10%), compared to Olink (51%, 23%) and MS-Seer (12%, 19%). The new assays in Olink Explore HT (absent in Explore3072) primarily drove its higher missingness and CV. The number of phenotypic associations varied by trait, while the number of genetic associations (*cis*-pQTLs at P<5e-08) were similar for Olink and SomaScan. Protein levels differed between ethnicities, with SomaScan identifying more ethnicity-differentiated proteins than Olink (FDR<0.05). Finally, SomaScan ANML normalization attenuated biologically relevant associations in our study. These findings underscore the importance of platform evaluation and data normalization strategies for application in large-scale, diverse population cohorts.

Introduction

Population-scale proteomics has heralded a new era in translational medicine, facilitating functional validation of genomic discoveries and gene target prioritization[1]. As a molecular phenotype, circulating proteins capture both genetic and environmental influences, providing insights into healthy and disease-perturbed pathways[2]. Large scale proteomic studies carried out in the UK Biobank[2], DeCODE[3], ARIC[4,5], and INTERVAL[6] studies have capitalized on proteomic profiling to identify robust biomarkers for incident disease, risk stratification and disease progression, and to identify potential therapeutic targets in novel pathways. Whilst these studies have furthered the pursuit of precision medicine[7], they are also notable for their focus on European and North American populations. There is a widely recognized need for comparable, well-powered studies in other global population groups, both as an opportunity to understand shared and population specific disease pathways, and to evaluate the generalizability of proteomic biomarkers across populations.

Mass spectrometry (MS) and multiplexed affinity-based assay methods have emerged as the two leading, complementary strategies for quantification of proteomic variation in samples from large-scale population-based studies. While MS has been considered the gold-standard for highly specific quantification of peptides, proteins, and proteoforms, many MS-based methods are recognized to have limited sensitivity, dynamic range and throughput[8,9]. State-of-the-art MS technologies such as the Orbitrap Astral (Thermo Fisher Scientific) and the timsTOF Pro (Bruker), have substantially improved assay performance, and may enable quantification of many thousands of plasma proteins from a single sample, especially when combined with innovative approaches to protein enrichment and depletion such as the Seer Proteograph or PreOmics ENRICH-iST[9]. Although preliminary results are encouraging[10,11], there is currently limited experience of these advanced MS-based approaches, and their suitability for use in large scale population studies remains to be determined.

In parallel, the aptamer-based SomaScan and antibody-based Olink assays have continuously improved their respective technologies, including increased depth and throughput. The most recent iterations of the SomaScan and Olink platforms can now assay 9,655 and 5,416 unique human proteins respectively, in a high-throughput and cost-effective manner. However, these ligand binding assays are recognized to have systematic differences in protein coverage, as well as specificity and reproducibility of their assays[12]. These differences in performance may contribute to limited cross-platform reproducibility, and impact biological insights. Furthermore, the performance of the newly added content in the latest generation of these affinity-based assays, has had limited technical or biological evaluation[11,13,14].

To advance understanding of disease pathways in the genetically, environmentally and culturally distinct populations of Asia, we have established a comprehensive longitudinal study (PRECISE-SG100K) comprising over 100,000 men and women living in South-East Asia. In preparation for planned proteomic profiling of all 100,000 participants, we carried out a pilot study, to evaluate the performance of the latest generation of MS and affinity-based assays.

Results

We performed a comparative analysis of the aptamer-based SomaScan 11K platform (SomaScan11K), the antibody-based Olink Explore HT platform (OlinkHT), and the Seer Proteograph XT workflow for nanoparticle-based enrichment coupled with data-independent acquisition by the Orbitrap Astral mass spectrometer (MS-Seer). The primary objective of our study was to evaluate their technical reproducibility, precision, specificity, and discovery potential for future large-scale application in our large multi-ethnic cohort, the PRECISE-SG100K study.

Study cohort characteristics

Plasma proteomic profiles were generated in 800 samples from 500 participants, adopting a design that included analysis of both technical as well as longitudinal replicates (**Figure 1**). All 800 samples were assayed using SomaScan11K, of which 516 samples from 216 participants were assayed using OlinkHT, and 100 samples from 50 participants were assayed using MS-Seer. Sample size varied because of limitations in resource availability, however, inclusion of overlapping samples provides opportunity for valuable orthogonal benchmarking. All MS-Seer samples were also analyzed by both SomaScan11K and OlinkHT. The study cohort included people of Chinese (East Asian), Indian (South Asian), and Malay (South-East Asian) background, with an average age of 51 ± 12 years, and 54% females. Further details of participant characteristics are shown in **Supplementary Table 1**.

Proteomic profiling by the three platforms

SomaScan11K returned results for 10,675 SOMAmers (mapping to 9,563 unique proteins as identified by UniProt IDs), while OlinkHT returned 5,405 features (5,401 UniProt IDs) and MS-Seer identified 5,945 protein groups (5,852 UniProt IDs). Overall, 12,825 unique proteins were identified by one or more of the three platforms (**Figure 1**). There were 3,718 proteins shared between SomaScan11K and OlinkHT, 3,845 shared between SomaScan11K and MS-Seer, and 2,168 shared between OlinkHT and MS-Seer. There were only 1,740 proteins common across all three platforms (**Supplementary Table 2**).

Data generated by each of the three platforms effectively distinguished between experimental and control samples (**Extended Data Figure 1a-g**). There were no obvious batch or plate effects (**Extended Data Figure 1h-n**). There were no outlier samples in the OlinkHT and MS-Seer data, and two outliers identified in the SomaScan11K data had not been assayed on OlinkHT or MS-Seer (**Extended Data Figure 2**). For OlinkHT and MS-Seer, the analyses were based on plate-scaled data. SomaLogic additionally apply a proprietary method called Adaptive Normalization by Maximum Likelihood (ANML) to their plate-scaled data, which normalizes measurements to a healthy U.S. population reference by iteratively estimating dilution-bin-specific scale factors from protein expression values within two standard deviations of the reference. The resulting scale factors are then applied to their respective SOMAmer reagents, to enhance technical performance and promote run-to-run consistency[15,16]. For SomaScan11K, we therefore had two sets of data: (i) pre-ANML, which is plate-scaled data; and (ii) ANML, which is the final normalized dataset recommended by SomaLogic that applies ANML in addition to plate-scaling. We evaluated the performance of both ANML and pre-ANML data for SomaScan11K.

131 **Technical performance**

132 In the SomaScan11K (500 samples and 10,675 aptamers) dataset, the median proportions of
133 proteins with measurements below the estimated limit of detection (LoD) per sample were 0.7%
134 (pre-ANML) and 2.6% (ANML). In contrast, a median of 11.8% of proteins for MS-Seer (46 samples
135 and 5,945 proteins) and 51.4% of proteins for OlinkHT (216 samples and 5,405 assays) had
136 measurements below LoD (**Figure 2a; Supplementary Figure 1**). At a threshold of ≤20% missingness
137 to define successful protein quantification, we found that 96% and 80% of proteins were
138 successfully called in the SomaScan11K and MS-Seer datasets. In contrast, only 40% of Olink assays
139 passed this permissive calling threshold (**Figure 2b**).

140 Coefficients of variations (CVs) between technical replicates showed that median intra- and inter-
141 plate CVs were lowest for the SomaScan11K assay, for both pre-ANML and ANML data (pre-ANML:
142 intra 7.9%, inter 9.1%; ANML: intra 4.6%, inter 5.2%; **Figure 2c**). In contrast, CVs for technical
143 replicates were higher for both OlinkHT (intra: 23.0%, inter: 23.0%) and MS-Seer (overall: 18.8%).
144 CVs for longitudinal samples collected 1 year apart were also higher for OlinkHT (28.3%) compared
145 to SomaScan11K (pre-ANML: 10.4%, ANML: 6.3%; **Supplementary Table 3**). Similarly, both
146 SomaScan11K pre-ANML and ANML exhibited higher correlation between technical replicates,
147 compared to OlinkHT and MS-Seer (**Figure 2d; Supplementary Figure 2**). Median pair-wise
148 correlation for protein concentrations across technical replicates was 0.80, 0.91, 0.67, and 0.52, for
149 SomaScan11K pre-ANML, ANML, OlinkHT, and MS-Seer, respectively (**Figure 2d**). Overall findings
150 remained unchanged when restricting these analyses to common samples (45 pairs) and common
151 proteins (1,740) across the three platforms (**Supplementary Figure 3**).

152 **Orthogonal confirmation**

153 Next, we calculated pairwise Spearman correlations for common proteins shared between
154 platforms (SomaScan11K and MS-Seer [3,845 proteins, 46 samples], OlinkHT and MS-Seer [2,168
155 proteins, 46 samples], and SomaScan11K and OlinkHT [3,718 proteins, 216 samples],
156 **Supplementary Table 4**). Median values for the correlation between the affinity-based assays and
157 MS-Seer assay were relatively low (SomaScan11K pre-ANML: 0.27, SomaScan11K ANML: 0.26,
158 OlinkHT 0.34; **Figures 3a-c; Supplementary Table 5**). More than half of the common proteins in
159 MS-Seer-SomaScan11K ANML (53.4%) and MS-Seer-OlinkHT (56.2%) comparisons had higher
160 correlations than the 99th-percentile of their null distributions, whereas the proportion was lower
161 for MS-Seer-SomaScan11K pre-ANML (38.1%).

162 The median correlations between SomaScan11K and OlinkHT were also low (pre-ANML: 0.16, ANML:
163 0.10; **Figures 3d,e; Supplementary Table 5**). There was a bimodal distribution in the correlations
164 with the largest peak at ~0.0 and a secondary peak at ~0.75, for both ANML and pre-ANML data
165 **(Figures 3d,e)**. For SomaScan11K-OlinkHT correlations, 44.7% of ANML and 48.5% of pre-ANML
166 proteins exceeded the 99th-percentile threshold of the null distribution, indicating that
167 approximately half of the overlapping proteins exhibit high cross-platform concordance.

168 **Phenotypic and genotypic associations**

169 Our analyses focused on the 216 samples with data for both SomaScan11K and OlinkHT using either
170 (1) all proteins assayed or (2) the common set of proteins assayed by both platforms. We found that
171 SomaScan11K pre-ANML data had the highest number of proteins associated with sex and BMI,
172 while OlinkHT had the highest number of associations with age (**Table 1a)**. For all three phenotypes,
173 we noted marked differences in the number of associations identified between SomaScan11K pre-
174 ANML and ANML data, especially for BMI (pre-ANML: 4,361, ANML: 1,234 associations at FDR<0.05;
175 **Table 1a; Supplementary Tables 6-7)**.

176 Cross-platform comparison of phenotypic associations including MS-Seer was limited in power
177 owing to the small number of common samples (n=46), with no detected associations with sex.
178 Known markers of sex, including leptin, sex-hormone binding globule, pregnancy zone protein, were
179 nominally associated across all three platforms at P<0.05. For age, and BMI, MS-Seer had the lowest
180 number of associations (age=11, BMI=50) compared to SomaScan11K (pre-ANML: age=17, BMI=237;
181 ANML: age=23, BMI=82) and OlinkHT (age=71, BMI=60) at FDR<0.05 (**Supplementary Tables 8-10**).

182 We also performed genome-wide association analysis for all analytes in SomaScan11K and OlinkHT
183 in the common set of 216 samples. Since SomaScan11K has multiple aptamers targeting the same
184 protein, we compared the number of unique proteins with at least one significant assay association,
185 to avoid overestimation. We found that SomaScan11K ANML identified the highest number of
186 proteins with at least one cis-pQTL (pre-ANML: 298, ANML: 351, OlinkHT: 300 at p<5e-08; **Table 1b**).
187 Approximately 45% of the cis-pQTLs identified by each platform are also reported as cis-eQTLs
188 (p<0.05) in the eQTLGen dataset[17]. Fine-mapping revealed a greater number of unique causal
189 variants for SomaScan11K compared to OlinkHT (pre-ANML: 123, ANML 142, OlinkHT: 117;
190 **Supplementary Table 11)**. Finally, SomaScan11K (both pre-ANML and ANML) identified a higher
191 number of proteins with trans-pQTLs (at p<5e-08/number of UniProt IDs) compared to OlinkHT
192 (**Table 1b**).

193 **Proteomic profiles vary between Asian ethnic groups**

194 Global PCA of all analytes across all samples for OlinkHT (5,405 analytes, 216 samples) and
195 SomaScan11K (pre-ANML and ANML, 10,675 analytes, 500 samples) data revealed that the Indian
196 and Malay proteomes were significantly different from that of the Chinese (Hotelling's T2 test
197 P<0.05; **Supplementary Table 12, Supplementary Figure 4**). Differences between the Indian and
198 Malay groups were also evident in the SomaScan11K dataset (N=500, **Supplementary Table 12**).
199 SomaScan11K identified a greater number of ethnicity-associated proteins compared to OlinkHT,
200 even in the common set of 216 samples (**Supplementary Table 13**). There were 191 proteins
201 robustly identified as ethnicity-differentiated across all three datasets (FDR <0.05 for at least one
202 pairwise comparison, and same direction of effect for the corresponding comparison across OlinkHT,
203 and SomaScan11K Pre-ANML and ANML data, **Supplementary Table 14**). Our analysis captured
204 proteins previously reported to vary across ancestries, such as Leptin, which was found to be highest
205 in Indians and lowest in Chinese, reflecting known differences in BMI and cardiovascular outcomes
206 between these ethnic groups[18,19]. It also identified ethnic differences in Lipopolysaccharide-binding
207 protein (LBP), a glycoprotein involved in immune response and atherogenesis[20,21]. LBP levels were
208 found to be higher in Indian and Malay individuals compared to the Chinese, and strongly positively

correlated with cardiovascular disease risk factors (BMI, C-reactive protein, triglyceride, and total cholesterol to high density lipoprotein ratio levels; **Supplementary Figure 5**).

Stratification by assay content

The SomaScan and Olink affinity-based platforms have both evolved in a stepwise manner to increase the number of proteins assayed. To understand how this might relate to assay performance, we compared results for SomaScan and Olink data, stratified by assay release (SomaScan sets 1 to 3: 5K assays, 7K minus 5K assays, 11K minus 7K assays; Olink sets 1 to 3: Explore 1536 assays, Explore 3072 minus Explore 1536 assays, Explore HT minus Explore 3072 assays; see **Methods**). We found that missingness and CV were consistently low, and that technical reproducibility was consistently high, across assay sets for SomaScan **(Supplementary Figure 6).** The number of phenotypic associations from each set of SomaScan was also proportional to the total number of proteins in each set, but a majority of the genotypic associations were from set 1 (**Supplementary Tables 15-16**). In contrast, we noted that missingness and CVs were progressively higher, and reproducibility progressively lower, for the newer Olink assay content. For example, missingness increased from 14.4% in set 1 to 76.7% in set 3, while CV increased from ~9% in set 1 to ~40% in set 3 **(Supplementary Table 17).** We also noted that there were fewer phenotypic and genotypic associations in the most recent Olink assay content. Irrespective of assay version, above-LoD proteins and higher-abundance proteins had better technical performance in both SomaScan and Olink platforms (**Supplementary Figures 7-9**).

Comparison between SomaScan11K pre-ANML and ANML data

From our technical and biological evaluations, we observed that the SomaScan11K ANML dataset generally has a lower CV, higher correlation between technical replicates, a higher number of age-associated proteins, and more pQTLs. However, the ANML data also show higher missingness, weaker orthogonal confirmation, and fewer associations with sex and BMI. We confirmed this through recalculation of genotypic and phenotypic associations using all 500 samples and 10,675 aptamers from the SomaScan11K platform for ANML and pre-ANML data. Even with this larger dataset, ANML retained a higher number of pQTLs and associations with age, whereas pre-ANML demonstrated significantly more associations with sex and BMI (**Supplementary Table 18**).

To evaluate the impact of ANML on data content, we first estimated the pair-wise Spearman correlation between our pre-ANML and ANML data. We found that 52.6% of proteins had a correlation below 0.8 (**Figure 4a**) between their pre- and post-ANML values, indicative of changes in the data structure owing to ANML scaling. We also observed that the ANML scaling factors strongly correlated with a range of phenotypes in our dataset, especially BMI, common cardiometabolic markers, and self-reported ethnicity (**Figure 4b, Extended Data Figure 3**), raising the possibility that ANML scaling factors are partly determined by physiological variation between participants. In keeping with this, we find that adiposity and related cardiometabolic phenotypes (e.g., CRP, BMI and insulin) were most predictive of ANML scaling factors when ranked based on their random forest-based Boruta feature selection method (**Extended Data Figure 4**).

Analysis of SomaLogic ANML normalization through data simulation

248 To investigate the impact of ANML scaling on associations between protein levels and phenotype,
249 we created synthetic relationships through spike-ins of the pre-ANML data (see **Methods**). The
250 synthetic relationships were designed to mimic associations with 20 different phenotypes, across a
251 plausible range of epidemiological effects. The 20 phenotypes were selected to include phenotypes
252 negatively, minimally or positively associated with ANML scaling factors (e.g. BMI, urea, and HDL,
253 respectively). We then compared the results for the associations of the spiked proteins with the
254 chosen phenotypes between the pre-ANML and ANML datasets.

255 We found that ANML led to a systematic shift in both the effect size and significance level of the
256 association between protein level and phenotype (**Figures 4c-f; Extended Data Figures 5-6;**
257 **Supplementary Figures 10-11**). In keeping with our initial hypothesis, the impact of ANML on the
258 association statistics appeared to mirror the magnitude and direction of the correlation between
259 the phenotypes and ANML scaling factors. For phenotypes that were highly negatively correlated
260 with ANML scaling factors (e.g. CRP, BMI), beta coefficients were consistently lower (more negative)
261 in the ANML analyses, to an extent that even reversed the direction of effect. Conversely,
262 phenotypes that were highly positively correlated with ANML scaling factors (e.g. HDL) became
263 higher (more positive). Phenotypes that showed only weak correlations with ANML scaling factors
264 (e.g. urea) were minimally affected by ANML normalization.

Discussion

We evaluated three proteomic platforms designed to deliver deep proteomic profiling suitable for population-scale studies. There were ~13,000 proteins quantified across the three platforms, however the overlap was only 1,740 proteins. As an initial key observation, we note that each platform measures a different fraction of the plasma proteome, indicating complementary information content for population studies.

Comparing technical performances, SomaScan11K had the lowest missingness, lowest CVs, and highest correlation between replicates, indicating stable and replicable measurements. OlinkHT's high missingness and high CVs were found to be primarily driven by the newest set of assays in their latest generation of the Explore panel. This observation is in agreement with another recent study that found the missingness and CV for the Olink Explore HT panel to be almost twice that of the Olink Explore 3072 panel[13]. These findings may be explained by the fact that the newer assays in Olink are largely representative of non-secretory proteins that might only present at very low levels in circulation unless in a specific disease state, leading to poor discoverability in generally healthy plasma and large variability in measurements using Olink's current method of quantification. MS-Seer, on the other hand, had acceptable data missingness, and modest precision reflected by its higher CVs and lower protein-wise correlation between replicates in comparison with SomaScan11K.

Pair-wise correlation for the limited set of shared proteins, revealed that OlinkHT had a higher median correlation with MS-Seer compared to SomaScan11K. We further observe that the correlation between OlinkHT and MS-Seer is significantly higher in the subset of older assays (equivalent to Olink Explore 1536), as well as in the above LoD subset of analytes. Correlation between Olink and SomaScan platforms have been widely discussed[13–15,22–24]. We compare data from the latest generations of these two platforms and find a median correlation of 0.16 (pre-ANML) and 0.10 (ANML), lower than previously reported[13,14]. However, the distribution of the correlation remained similar to previous reports consisting of a bimodal curve with two peaks – one at 0.0, and the other at 0.75. When restricting the analysis to data above LoD for each platform, we find that the correlation between Olink and SomaScan increases to 0.46 (pre-ANML) and 0.43 (ANML).

We evaluated phenotypic and genotypic associations with common phenotypes such as age, sex, BMI. We find that above LoD analytes contribute to a majority of the associations for both OlinkHT and SomaScan11K. Overall, OlinkHT has a greater number of age-specific markers while SomaScan11K yields more sex- and BMI-specific markers. This may reflect differences in the composition of each platform's marker panel, with each capturing a distinct subset of the proteome. We observe a similar number of proteins with *cis*-pQTL signals across the two platforms, however, *trans*-pQTL discovery was higher in SomaScan11K compared to OlinkHT. The number of *trans*-pQTLs discovered for SomaScan is relatively high given the limited sample size of 216[2], raining the possibility of protein-protein interactions or off-target effects. Further studies are needed to better understand the nature of the *trans*-pQTLs.

We noted substantial differences in the distribution of protein levels and association test results, between the SomaScan11K pre-ANML and ANML data, in agreement with previous reports[15,23,24].

304 The ANML method aims to adjust for unwanted technical variations and reduce batch effects in
305 large-scale proteomic studies - the reference population for which may not reflect the ethnic
306 diversity of the SG100K cohort[25]. We find that for 52.6% of the proteins, pre-ANML and ANML
307 concentrations are only weakly correlated. We show that ANML scaling factors are correlated with
308 ethnicity, adiposity and multiple cardiometabolic phenotypes, and that ANML normalization
309 systematically shifts data distributions, with the correlation between the phenotype and the ANML
310 scaling factor predicting the extent and direction of this effect on phenotypic associations.
311 Additionally, pre-ANML data demonstrates higher orthogonal confirmation in our data, consistent
312 with prior studies reporting higher correlation between pre-ANML and Olink data compared to
313 ANML data[15,23]. Our evaluation of the effect of ANML normalization on biological discovery extends
314 on these observations, providing valuable insights and suggesting that while ANML normalization
315 may improve technical metrics, it may also be removing biological signals from datasets.

316 Our comparative analysis finds that the SomaScan11K assay (both pre-ANML and ANML) has lower
317 missingness and higher reproducibility than OlinkHT and MS-Seer assays - two critical measures of
318 technical performance. We observe that many of the new OlinkHT assays have poorer technical
319 performance than the assays in Olink's earlier generation Explore panels. While OlinkHT and
320 SomaScan11K exhibit distinct strengths in biological discovery, we identify more proteins with
321 ethnicity-associated differences using SomaScan11K than OlinkHT. Additionally, we demonstrate
322 that ANML normalization, a proprietary algorithm applied by SomaLogic as the final step in their
323 data generation, may be removing biologically relevant signals. Nevertheless, we note that the three
324 platforms continue to have largely non-overlapping content, indicating that population-scale studies
325 are likely to benefit from the implementation of a combination of technologies to maximize
326 discovery potential. Our findings will enable rationale design and platform selection for proteomic
327 studies focussed on advancing identification of biomarkers and disease pathways that are relevant
328 to global populations.

329 # Methods

330 ## Study design

331 Baseline samples from 216 participants were randomly selected from the PRECISE-SG100K cohort
332 (https://www.npm.sg/partners/precise-sg100k/) to be run on two different platforms: Olink Explore
333 HT and SomaScan 11K Assay. For 100 of these samples, three technical replicates were included in
334 the study, as well as a longitudinal sample collected during a follow-up visit, approximately a year
335 later. An additional 284 baseline samples selected randomly from the cohort were run on the
336 SomaScan platform. Of the 100 baseline samples with replicates, a random subset of 50 baseline
337 samples in duplicates were run on the Thermo Fisher Orbitrap Astral Mass Spectrometer (MS)
338 instrument coupled with Seer Proteograph XT workflow. Thus, a total of 516 samples were run using
339 Olink Explore HT, 800 samples using SomaScan 11K, 100 samples using Orbitrap Astral MS.

340 All assays were carried out in EDTA plasma separated from venous whole blood, collected from
341 participants in the fasting state. Blood samples were collected by a certified phlebotomist, during
342 the morning of the participant's visit. Samples were centrifuged within four hours and plasma was
343 stored at -80 degrees Celsius before analysis. The overall study samples were selected such that
344 they were age-, sex-matched across the three ethnic groups, i.e., Chinese, Indian and Malay.
345 Samples were randomized across plates. For samples with replicates, two technical replicates were
346 on the same plate to enable assessment of intra-plate CVs, and the third technical replicate was on
347 a different plate to enable inter-plate CVs. Longitudinal replicates were on the same plate as the
348 third technical replicate to enable longitudinal CVs. It was also ensured that replicates were not
349 adjacent to each other.

350 ## Aptamer-based proteomics platform

351 800 samples from 500 participants from PRECISE-SG100K, along with 32 buffer samples (without
352 added sample), 50 calibrators, and 30 QC samples (provided by SomaLogic from pooled healthy
353 donor controls), divided into 10 plates from 2 batches, were analyzed using the SomaScan 11K Assay
354 v5.0[26] (*SomaLogic, Inc.*) at the SomaLogic Boulder Lab. This assay comprises 10,776 SOMAmers,
355 which mapped to 9,655 UniProt IDs provided by SomaLogic; the remaining SOMAmers are controls,
356 including hybridization control elution SOMAmers used in normalization and others targeting non-
357 human proteins. To cover a broad range of protein concentrations, SOMAmers are grouped into
358 dilution bins of 1:5, 1:200, and 1:20,000. Each sample required 130 µL of human plasma. Data
359 processing, normalization, and quality control were conducted by SomaLogic, following sequential
360 procedures including hybridization normalization, plate scaling and calibration[27]. SomaLogic also
361 applied additional adaptive normalization by maximum likelihood (ANML) to the QC and
362 experimental samples. To understand how ANML influences SomaScan11K data, we included both
363 pre-ANML and ANML data in our comparison. One buffer sample failed QC evaluation and was
364 excluded; all experimental samples passed QC. For all analysis, we used log2-transformed relative
365 fluorescence units (RFU) for SomaScan11K data.

366 ## Antibody-based proteomics platform

367 Antibody-based proteomic profiling was performed at the Olink Singapore Lab using the Olink
368 Explore HT platform[28] (*Olink Proteomics*). This assay employs proximity extension assay technology
369 to measure 5,420 analytes (mapped to 5,416 UniProt IDs provided by Olink) using only 2 µL of
370 plasma. To encompass a broad range of protein abundances, assays were grouped into dilution
371 series of 1:1, 1:10, 1:100, 1:1,000, and 1:100,000. A total of 516 samples from 216 participants from
372 PRECISE-SG100K were analyzed. The 60 external control samples (including 12 negative controls, 30
373 plate controls, and 18 sample controls from Olink), along with experimental samples, were
374 distributed across 6 plates in 3 batches. Three types of internal controls—incubation control,
375 extension control, and amplification control—were added to all samples. Two samples were
376 excluded due to QC failure. Normalized Protein eXpression (NPX) values were then generated in two
377 main steps: first, sequencing counts of each assay in a sample were divided by the extension control
378 count for that sample and log2-transformed; second, intensity normalization was performed by
379 subtracting the median of the experimental samples within each plate for each assay.

380 **Mass spectrometry-based proteomics platform**

381 MS-based untargeted proteomic profiling using the Seer Proteograph XT workflow[10] (*Seer, Inc.*)
382 coupled with the Orbitrap Astral MS instrument[29] (*Thermo Fisher Scientific*) was performed at the
383 Seer Redwood Lab. All samples—including 100 plasma samples from 50 participants from PRECISE-
384 SG100K and 15 pooled plasma replicates from Seer - were processed (each sample was diluted from
385 120 µL to a total input volume of 240 µL for processing) on a Seer SP100 automation instrument
386 across three Proteograph XT Assay plates; five samples were lost due to trypsin dispensing errors.
387 Peptides were then separated using a Thermo Scientific Vanquish Neo UHPLC system under
388 nanoflow conditions at 1,000 nL/min with a 21-minute gradient. Mass spectrometry analysis was
389 conducted in data-independent acquisition mode on the Orbitrap Astral instrument, using a 400-ng
390 injection amount and a total acquisition time of 26 minutes per run. Each sample was run twice
391 within each plate: once with XT Nanoparticle Suspension A and once with Suspension B.

392 **Mass spectrometry data processing**

393 MS raw data were processed using DIA-NN[30] (version 1.8.1) with a library-free search based on the
394 Homo sapiens UniProt reference database (accessed December 2022). Peptide and protein
395 intensities were quantified in match-between-runs mode using the following flags: `--mass-acc-ms1`
396 `3, --mass-acc 8, --qvalue 0.01, --matrices, --missed-cleavages 1, --met-excision, -`
397 `-cut K*,R*, --smart-profiling, --relaxed-prot-inf, --reannotate, --peak-center, --`
398 `no-ifs-removal`. Raw precursor intensities from DIA-NN were then normalized using calibration
399 peptides spiked into each sample prior to MS injection and aggregated to protein intensities using
400 the MaxLFQ algorithm in the iq R package[31], keeping precursors from different nanoparticles
401 separate. Plate-level batch effects were corrected using the removeBatchEffect function from the
402 limma R package[32]. Further preprocessing includes log2-transformation and missing value
403 imputation using a sequential k-nearest neighbors (KNN) algorithm[33]. While MS-Seer provides
404 additional peptide-level information for each protein, it was not used in this study to enable direct
405 comparison between three platforms.

406 **Limit of detection and missingness**

407 Limit of detection (LoD) is defined as the lowest protein concentration likely to be reliably
408 distinguished from analytical noise (i.e., the signal produced in the absence of protein)[34]. For LoD
409 calculations, we adopted the formulae recommended by each platform, using readouts from blank
410 samples. For SomaScan data, the LoD was calculated as Median (Blank) + 4.9 * MAD (Blank). For
411 Olink data, the LoD was derived as Median (Blank) + 3 * SD (Blank) or Median (Blank) + 0.2,
412 whichever value is highest, using function called olink_lod function from OlinkAnalyze R package.
413 The proportion of data below LoD is termed as missingness.

414 To enable fair comparison between platforms, we also applied consistent formulae based on the
415 Clinical and Laboratory Standards Institute (CLSI) definitions[34] to compare the overall proportion of
416 measurements below the LoD for each platform. These formulae included: Formula 1: LoD = Mean
417 (Blank) + 3.3 * SD (Blank); and Formula 2: LoD = Mean (Blank) + 1.65 * SD (Blank) + 1.65 * SD (Lowest
418 5% samples).

419 For the MS data, proteins were identified and quantified only if they met an FDR threshold of less
420 than 1%; otherwise, they were recorded as NA. In our analysis, we considered missing values as
421 equivalent to measurements below the LoD.

422 For sample-level missingness, we estimated the proportion of analytes with measurements below
423 LoD for each sample, and reported the distribution and median missingness across all samples. For
424 protein-level missingness, we estimated the proportion of samples with measurements below LoD
425 for each analyte, and reported the numbers of analytes with missingness at or beyond specific levels
426 (= 0%, > 20%, > 50% and = 100%). The primary analyses were conducted using all samples (both the
427 first technical replicates and single samples [those without replicates]) and all analytes available for
428 each platform. For LoD-based stratified analyses, we categorized the analytes being measured in
429 each platform as Above LoD or Below LoD based on a 20% threshold, i.e., if an analyte was below
430 LoD (or missing) in more than 20% samples, it was classified as Below LoD and vice-versa.

431 **Technical reproducibility**

432 For SomaScan11K and OlinkHT, to assess technical reproducibility at the sample level, for each
433 sample with triplicates, we calculate the mean pairwise Pearson correlation among technical
434 replicates. At the protein level, each protein is measured in triplicate across 100 samples, producing
435 three 100-by-1 measurement vectors. We then compute the average pairwise Pearson correlations
436 among these vectors to obtain the protein-level mean Pearson correlation. The above method also
437 applies to MS-Seer data, but only 50 samples have duplicates in this case.

438 **Coefficient of variation (CV)**

439 We estimated the coefficients of variation (CVs) for technical/longitudinal replicates on the same
440 plate (intra-) and different plates (inter-) for the affinity-based platforms (SomaScan11K and
441 OlinkHT). The CVs for MS-Seer platform were calculated based on technical replicates irrespective
442 of intra/inter-plate runs. The formula used for CV calculation for each platform are as follows:

443 SomaScan11K: $CV_{ijk} = 100 \times \sqrt{e^{(\log 2 \times SD(log2(RFU)))^2} - 1}$

444 OlinkHT: $CV_{ijk} = 100 \times \sqrt{e^{(\log 2 \times SD(NPX))^2} - 1}$

445 MS-Seer: $CV_{ijk} = 100 \times \sqrt{e^{(\log 2 \times SD(log2(Relative\ Intensity)))^2} - 1}$

446 The CVs for each analyte were then averaged across all samples (with technical/longitudinal
447 replicates) to obtain a single CV for each analyte being measured. We then looked at the distribution
448 of these CVs for each platform and reported the CV quantiles. The CVs were calculated for all
449 samples and all analytes available for each platform and also for only the common samples and
450 common analytes shared by all the three platforms.

451 **Correlation between platforms**

452 We compared two proteomic platforms by examining protein-wise correlations for a set of shared
453 proteins measured in common samples. Proteins were aligned across platforms based on their
454 provided UniProt identifiers, ensuring that only columns corresponding to the same protein in both
455 datasets were compared. Spearman's rank correlation coefficient was then calculated for each
456 matched protein pair, providing a measure of the agreement between the platforms. The
457 distribution of this calculated correlation for all common proteins between the platforms gives us
458 the observed correlation distribution. To establish a background distribution of correlation values,
459 we performed a permutation-based null experiment in which the protein labels for one platform
460 were shuffled randomly, and Spearman correlations were recalculated for each protein under this
461 randomized mapping. This procedure was repeated 1,000 times, giving us a distribution of
462 correlation values expected under random pairing. The mean of these permuted correlations serves
463 as the background correlation estimate. Observed correlations surpassing the 99th percentile of the
464 background distribution was considered indicative of a strong association between the two
465 platforms.

466 **Phenotypic association analysis**

467 We evaluated the association of proteins with three key phenotypes: age, sex, and BMI, using
468 generalized linear regression models, adjusting for ethnicity and the two other phenotypes not
469 being tested. Age and BMI were rank inverse-normal transformed prior to association tests. We also
470 evaluated the number of phenotypic associations stratified by above/below LoD proteins and assay
471 sets as described previously (for SomaScan11K and OlinkHT). This analysis was performed across all
472 proteins and common samples, as well as common proteins and common samples, for the two
473 affinity-based platforms (SomaScan11K and OlinkHT). When comparing the associations for ANML
474 data with pre-ANML data, we calculated the associations using all 500 samples and 10,675 aptamers.

475 **Genotypic association analysis**

476 We performed GWAS using 30X whole-genome sequencing data[35], filtering variants for missingness
477 <2%, minor allele frequency (MAF) >0.05, and Hardy-Weinberg equilibrium p-value $>1\times10^{-6}$.
478 Association testing was conducted on 197 samples using the linear mixed model implemented in
479 GCTA-fastGWA[36], adjusting for age, sex, and the top 20 genetic principal components. Protein
480 expression levels were rank-based inverse normal transformed prior to analysis.

481 To identify independent association signals, we applied LD-based clumping to GWAS summary
482 statistics using PLINK[37] with a p-value threshold = 5×10^{-8}, LD-R^2 threshold of 0.01 within a 1Mb
483 window around index variants. Independent genetic variants were classified as *cis* if they were
484 located within ±1 Mb of the gene body encoding the corresponding protein, and *trans* otherwise. A
485 genome-wide significance threshold of $p < 5\times10^{-8}$ was used for identifying *cis* associations. For *trans*
486 associations, Bonferroni correction was applied based on the number of proteins tested: $p <$
487 5.2×10^{-12} for SomaScan11K (9,563 UniProt IDs) and $p < 9.2\times10^{-12}$ for OlinkHT (5,401 UniProt IDs). To
488 control for multiple analytes targeting the same protein, we also report the number of unique
489 proteins with at least one significant association, i.e. one analyte per UniProt ID. For this, we
490 selected the analyte with the maximum number of associations or a random analyte in case of ties.
491 We also evaluated the number of genotypic associations stratified by above/below LoD proteins
492 and assay sets as described previously (for SomaScan11K and OlinkHT). To allow for a fair
493 comparison, we also analyzed the number of associations for only common samples and common
494 proteins across SomaScan11K and OlinkHT. When comparing the ANML data with pre-ANML data,
495 we calculated the number of genotypic associations using all 500 samples and 10,675 aptamers.

496 **Fine-mapping of *cis*-pQTLs**

497 We performed statistical fine-mapping using **SuSiE-X**[38] (single population) to identify putative causal
498 associations. For each lead protein-SNP pair, we extracted summary statistics for all variants within
499 a 1.5Mb window centered on the sentinel variant. Fine-mapping was performed for each locus, with
500 the credible set coverage level set to 90% and p-value threshold of 5e-08. Linkage disequilibrium
501 (LD) matrices were computed from the same genotype data used for the GWAS.
502 Credible sets were reported if the posterior inclusion probability (PIP) exceeded the defined
503 threshold (>0.90) and the model converged successfully. Variants within the credible sets with PIP
504 >0.5 were classified as causal variants for the specific protein.
505

506 **Concordance of *cis*-pQTL and *cis*-eQTL associations**

507 We queried the cis-pQTLs against the eQTLGen[17] Phase 1 dataset to identify overlapping signals that
508 were also reported as cis-eQTLs for the same gene. We first merged the datasets based on variant
509 position and gene identifier, and subsequently applied a cis-eQTL significance threshold of $p <0.05$.

510 **Spike-in simulation procedure**

511 Twenty quantitative phenotypes with different levels of Spearman correlation with ANML scaling
512 factor in the largest dilution bin (1:5) were selected first, including C-reactive protein (CRP), Insulin,
513 Body mass index (BMI), Triglyceride, Bone Mineral Density (BMD)-Hip, Alanine aminotransferase
514 (ALT), Gamma-glutamyl transpeptidase (GGT), Waist hip rate (WHR), Systolic blood pressure (SBP),
515 Glucose, Total cholesterol, Albumin, Uric acid, BMD-Lumbar, Age, Urea, Creatinine, Na, Cl and High
516 density lipoprotein (HDL). Then for each phenotype, we generated 100 synthetic proteins (50 with
517 positive effect size and 50 with negative) with p-values ranging from 1e-0.5 to 1e-20. To minimize
518 the influence on sample distribution, the chosen proteins from the 1:5 dilution bin to replace have
519 the same direction of effect size (positive or negative). And data for 100 synthetic proteins were
520 replaced in the pre-ANML SomaScan11K data under their original column names while keeping

521 other columns unchanged. Altogether, we developed 2 methods to generate synthetic proteins
522 (details described below) and generated 40 datasets (2 methods × 20 phenotypes), with each file
523 containing 100 synthetic data columns. Finally, SomaLogic helped to run ANML on these new
524 datasets and we checked how ANML influences the effect size beta and p-value in linear regression
525 (phenotype ~ each simulated protein).

526 **Simulation method 1**

527 We generated synthetic proteins for each phenotype with desired correlations between the protein
528 RFUs and target phenotypes by reshuffling the sample rows in the original pre-ANML data. First,
529 protein RFU ranks were either perfectly aligned with the phenotype ranks (Spearman $\rho = 1$) or
530 aligned in the exact opposite direction of the phenotype (Spearman $\rho = -1$) depending on the desired
531 direction of association. To decrease this correlation and control the p-values for linear regression,
532 a specified fraction (e.g., 10%, 25%, 50%, 80%, 90%) of these ranks were randomly shuffled. To avoid
533 perfect linearity between the remaining unshuffled ranks and the phenotype, and to introduce
534 realistic variability, we added minor, random noise to these unshuffled values. This noise was scaled
535 relative to the standard deviation of the $\log_2$-transformed protein intensities using a defined factor
536 (0.25) so that the magnitude of the noise was strong enough to remove the residual linearity in the
537 unshuffled data. Using the above-described method, we generated 50 proteins with positive and 50
538 with negative association with each target phenotype, with the desired degree of correlation, while
539 also preserving the distribution pattern of the original protein columns that were replaced.

540 **Simulation method 2**

541 For each phenotype, inverse normal transformation was applied firstly to derive $Z_{Phenotype}$ which
542 follows a standard normal distribution. Next, a target Pearson correlation ρ was set. Given
543 $Z_{Phenotype}$, we generated $Z_{Protein}$ from a normal distribution with mean $\rho\, Z_{Phenotype}$ and variance $1-\rho^2$.
544 Then by probability theorem, $Z_{Protein}$ follows a standard normal distribution and has Pearson
545 correlation ρ with $Z_{Phenotype}$. We then mapped $Z_{Protein}$ to the distribution of one original protein in
546 pre-ANML data (by mapping the quantiles) and obtained a simulated protein with correlation
547 close to ρ with $Z_{Phenotype}$. Using this method, we generated simulated proteins for each phenotype
548 while controlling for the linear regression p-value and target Pearson correlation ρ, and preserving
549 the distribution pattern of the original protein columns that were replaced.

550 **Analysis of ethnic differences**

551 R function *prcomp* was used to perform PCA of proteomic data. Hotelling's T2 test for multivariate
552 pairwise comparison was used to estimate significant differences in the means of principal
553 components 1 to 5 for each pair of ethnicities. Linear regression adjusting for age and sex was
554 used to determine association of each analyte with ethnicity, and a significance threshold of
555 FDR<0.05 was applied to each pairwise comparison (Indian vs Chinese, Malay vs Chinese, and
556 Malay vs Indian). For the protein P18428 (LBP), we estimated pairwise Spearman correlation with
557 9 clinical variables BMI, mean systolic and diastolic blood pressure (mean SBP and mean DBP), C-
558 reactive protein (CRP), triglyceride (Trig), total cholesterol (TC), high density lipoprotein (HDL), low
559 density lipoprotein (LDL) and TC to HDL ratio. Correlation analysis was performed for protein

560 measured by OlinkHT, SomaScan11K Pre-ANML, and SomaScan11K ANML, and a p-value threshold
561 of 0.005 (correcting for the 9 tests) was applied to each set of analysis.

562 **Bioinformatics and statistical analyses**

563 For all analyses, we excluded assays with multiple UniProt IDs, non-human or contaminant proteins,
564 and internal control proteins. Outlier detection was conducted using four criteria: PCA (PC1 & PC2),
565 sample median, sample IQR, and mean Pearson correlation with other samples. Samples deviating
566 more than five standard deviations from the mean in any of these metrics were considered outliers.
567 For technical evaluations involving common proteins across platforms, we retained only one
568 representative analyte (one with the lowest proportion below LoD) for protein whose UniProt ID
569 corresponds to multiple analytes. Pearson correlation was used for within-platform technical
570 metrics whereas Spearman correlation was used for between-platform comparison.

571 We also stratified the analysis based on the different release generations of the platforms: For
572 SomaScan11K, the SOMAmers were divided into three sets: (set 1) assays in SomaScan 5K, (set 2)
573 assays in SomaScan 7K minus assays in SomaScan 5K, and (set 3) assays in SomaScan 11K minus
574 assays in SomaScan 7K. For OlinkHT, the three sets were: (set 1) assays in Olink Explore 1536, (set 2)
575 assays in Olink Explore 3072 minus assays in Olink Explore 1536, and (set 3) assays in Olink Explore
576 HT minus assays in Olink Explore 3072. The analysis was also stratified by the missingness of proteins,
577 with above-LoD proteins defined as proteins measured in 80% or more samples and below-LoD
578 proteins defined as proteins missing in more than 20% samples.

579 ANML scaling factors were derived by dividing post-ANML protein RFU by the corresponding pre-
580 ANML protein expression on the original scale, yielding one scale factor for each sample–protein
581 pair. As these factors are highly similar among proteins within a given dilution bin, the median value
582 within each bin was employed as the representative scaling factor for all proteins in that bin.

583 The relative contributions of all 29 phenotypes to ANML scaling factor prediction were assessed
584 using a random forest–based Boruta feature selection procedure. By iteratively comparing the
585 importance scores of each actual phenotype against those of randomized shadow features, Boruta
586 robustly identified the subset of phenotypes whose importance significantly exceeded that of noise.
587 The confirmed features thus highlight the key traits driving ANML scaling factor estimation.

Data and code availability

Researchers may apply for access to individual level data through the study Data Access Committee (email: helios_science@ntu.edu.sg). All summary data have been made available in the supplementary tables. The R and Python scripts for analysis and visualization are available via GitHub.

Acknowledgements

We would like to express our gratitude to the HELIOS operational team for sample collection and processing, and sample retrieval and dissemination for this project. We would also like to thank the National Precision Medicine Programme for sharing relevant whole genome sequence data. This study is supported by Singapore Ministry of Health's (MOH) National Medical Research Council (NMRC) under its OF-LCG funding scheme (MOH-000271-00), Singapore Translational Research (StaR) funding scheme (NMRC/StaR/0028/2017), the National Research Foundation, Singapore through the Singapore MOH NMRC and the Precision Health Research, Singapore (PRECISE) under the National Precision Medicine programme (NMRC/PRECISE/2020) and intramural funding from Nanyang Technological University, Lee Kong Chian School of Medicine and the National Healthcare Group. This research was also supported in part through the National Research Foundation, Prime Minister's Office, Singapore under its Campus for Research Excellence and Technological Enterprise (CREATE) programme. N.S and J.C.C had full access to all the data in this study and take responsibility for the integrity of the data and the accuracy of the data analysis.

Author Contributions Statement

J.C.C and N.S conceived and designed the study. A.B and H.W processed the proteomic data. A.B, H.W, P.R.J, N.S performed data analyses. A.B, H.W, P.R.J, J.C.C, N.S wrote the manuscript. L.D.W, O.B, Z.D, J.F, J.N, J.Lee, E.R, J.Liu, S.MS, E.P, CY.C, B.L, S.S.J, N.B, C.B, M.L, W.Z, X.S, P.T provided critical feedback on data analysis, interpretation of results, and writing of manuscript. All authors reviewed and contributed to the revision of the submitted manuscript.

Competing Interests Statement

L.D.W works for Alnylam Pharmaceuticals and does not hold stocks as part of employment. O.B works for Bayer AG and does not hold stocks as part of employment. Z.D works for Boehringer Ingelheim Pharma GmbH & Co. KG and does not hold stocks as part of employment. J.F works for Novo Nordisk A/S and holds minor share portions as part of employment. The rest of the authors declare no competing interests.

622 **References**

623 1. Sun, B. B., Suhre, K. & Gibson, B. W. Promises and Challenges of populational Proteomics in
624 Health and Disease. *Mol. Cell. Proteomics* **23**, (2024).
625 2. Sun, B. B. *et al.* Plasma proteomic associations with genetics and health in the UK Biobank.
626 *Nature* **622**, 329–338 (2023).
627 3. Ferkingstad, E. *et al.* Large-scale integration of the plasma proteome with genetics and disease.
628 *Nat Genet* **53**, 1712–1721 (2021).
629 4. Shah, A. M. *et al.* Large scale plasma proteomics identifies novel proteins and protein networks
630 associated with heart failure development. *Nat. Commun.* **15**, 528 (2024).
631 5. Rooney, M. R. *et al.* Proteomic Predictors of Incident Diabetes: Results From the Atherosclerosis
632 Risk in Communities (ARIC) Study. *Diabetes Care* **46**, 733–741 (2023).
633 6. Sun, B. B. *et al.* Genomic atlas of the human plasma proteome. *Nature* **558**, 73–79 (2018).
634 7. Kurgan, N., Kjærgaard Larsen, J. & Deshmukh, A. S. Harnessing the power of proteomics in
635 precision diabetes medicine. *Diabetologia* **67**, 783–797 (2024).
636 8. Hendricks, N. G. *et al.* An Inflection Point in High-Throughput Proteomics with Orbitrap Astral:
637 Analysis of Biofluids, Cells, and Tissues. *J. Proteome Res.* **23**, 4163–4169 (2024).
638 9. Soni, R. K. Frontiers in plasma proteome profiling platforms: innovations and applications. *Clin.*
639 *Proteomics* **21**, 43 (2024).
640 10. Suhre, K. *et al.* Nanoparticle enrichment mass-spectrometry proteomics identifies protein-
641 altering variants for precise pQTL mapping. *Nat. Commun.* **15**, 989 (2024).
642 11. Pietzner, M. *et al.* Nanoparticle enriched mass spectrometry proteomics in British South
643 Asians identifies novel variant-protein-disease mechanisms. 2025.08.12.25333522 Preprint at
644 https://doi.org/10.1101/2025.08.12.25333522 (2025).

645 12. Suhre, K., McCarthy, M. I. & Schwenk, J. M. Genetics meets proteomics: perspectives for
646 large population-based studies. *Nat Rev Genet* **22**, 19–37 (2021).
647 13. Kirsher, D. Y. *et al.* The Current Landscape of Plasma Proteomics: Technical Advances,
648 Biological Insights, and Biomarker Discovery. 2025.02.14.638375 Preprint at
649 https://doi.org/10.1101/2025.02.14.638375 (2025).
650 14. Rooney, M. R. *et al.* Correlations Within and Between Highly Multiplexed Proteomic Assays
651 of Human Plasma. *Clin. Chem.* **71**, 677–687 (2025).
652 15. Eldjarn, G. H. *et al.* Large-scale plasma proteomics comparisons through genetics and
653 disease associations. *Nature* **622**, 348–358 (2023).
654 16. Williams, S. A. *et al.* Plasma protein patterns as comprehensive indicators of health. *Nat.*
655 *Med.* **25**, 1851–1857 (2019).
656 17. U, V. *et al.* Unraveling the polygenic architecture of complex traits using blood eQTL
657 metaanalysis. (2018).
658 18. Shamsuzzaman, A. S. M. *et al.* Independent Association Between Plasma Leptin and C-
659 Reactive Protein in Healthy Humans. *Circulation* **109**, 2181–2185 (2004).
660 19. Mente, A. *et al.* Ethnic Variation in Adiponectin and Leptin Levels and Their Association
661 With Adiposity and Insulin Resistance. *Diabetes Care* **33**, 1629–1634 (2010).
662 20. Lepper, P. M. *et al.* Lipopolysaccharide-binding protein (LBP) is associated with total and
663 cardiovascular mortality in individuals with or without stable coronary artery disease--results
664 from the Ludwigshafen Risk and Cardiovascular Health Study (LURIC). *Atherosclerosis* **219**, 291–
665 297 (2011).
666 21. Sallam, T. *et al.* The macrophage LBP gene is an LXR target that promotes macrophage
667 survival and atherosclerosis. *J. Lipid Res.* **55**, 1120–1130 (2014).

668 22. Katz, D. H. *et al.* Proteomic profiling platforms head to head: Leveraging genetics and
669 clinical traits to compare aptamer- and antibody-based methods. *Sci Adv* **8**, eabm5164 (2022).
670 23. Wang, B. *et al.* Comparative studies of 2168 plasma proteins measured by two affinity-
671 based platforms in 4000 Chinese adults. *Nat. Commun.* **16**, 1869 (2025).
672 24. Pietzner, M. *et al.* Synergistic insights into human health from aptamer- and antibody-
673 based proteomic profiling. *Nat Commun* **12**, 6822 (2021).
674 25. Williams, S. A. *et al.* Plasma protein patterns as comprehensive indicators of health. *Nat.*
675 *Med.* **25**, 1851–1857 (2019).
676 26. Gold, L. *et al.* Aptamer-Based Multiplexed Proteomic Technology for Biomarker Discovery.
677 *PLoS ONE* **5**, e15004 (2010).
678 27. Candia, J., Daya, G. N., Tanaka, T., Ferrucci, L. & Walker, K. A. Assessment of variability in
679 the plasma 7k SomaScan proteomics assay. *Sci. Rep.* **12**, 17147 (2022).
680 28. Wik, L. *et al.* Proximity Extension Assay in Combination with Next-Generation Sequencing
681 for High-throughput Proteome-wide Analysis. *Mol. Cell. Proteomics MCP* **20**, 100168 (2021).
682 29. Guzman, U. H. *et al.* Ultra-fast label-free quantification and comprehensive proteome
683 coverage with narrow-window data-independent acquisition. *Nat. Biotechnol.* 1–12 (2024)
684 doi:10.1038/s41587-023-02099-7.
685 30. Demichev, V., Messner, C. B., Vernardis, S. I., Lilley, K. S. & Ralser, M. DIA-NN: neural
686 networks and interference correction enable deep proteome coverage in high throughput. *Nat.*
687 *Methods* **17**, 41–44 (2020).
688 31. Pham, T. V., Henneman, A. A. & Jimenez, C. R. iq: an R package to estimate relative protein
689 abundances from ion quantification in DIA-MS-based proteomics. *Bioinformatics* **36**, 2611–2613
690 (2020).

691 32. Ritchie, M. E. *et al.* limma powers differential expression analyses for RNA-sequencing and
692 microarray studies. *Nucleic Acids Res.* **43**, e47 (2015).
693 33. Wang, S. *et al.* NAguideR: performing and prioritizing missing value imputations for
694 consistent bottom-up proteomic analyses. *Nucleic Acids Res.* **48**, e83 (2020).
695 34. Armbruster, D. A. & Pry, T. Limit of Blank, Limit of Detection and Limit of Quantitation. *Clin.*
696 *Biochem. Rev.* **29**, S49–S52 (2008).
697 35. Wang, X. *et al.* The Health for Life in Singapore (HELIOS) Study: delivering Precision
698 Medicine research for Asian populations. Preprint at
699 https://doi.org/10.1101/2024.05.14.24307259 (2024).
700 36. Jiang, L. *et al.* A resource-efficient tool for mixed model association analysis of large-scale
701 data. *Nat. Genet.* **51**, 1749–1755 (2019).
702 37. Purcell, S. *et al.* PLINK: a tool set for whole-genome association and population-based
703 linkage analyses. *Am. J. Hum. Genet.* **81**, 559–575 (2007).
704 38. Wang, G., Sarkar, A., Carbonetto, P. & Stephens, M. A Simple New Approach to Variable
705 Selection in Regression, with Application to Genetic Fine Mapping. *J. R. Stat. Soc. Ser. B Stat.*
706 *Methodol.* **82**, 1273–1300 (2020).
707

Tables

Table 1. Comparison of phenotypic and genotypic associations for SomaScan11K pre-ANML, SomaScan11K ANML and OlinkHT. (a) The total number of associations (FDR < 0.05) with Age, Sex, and BMI. (b) The total number of *cis*-pQTLs (p<5e-08), and *trans*-pQTLs (p<5e-08/number of UniProt IDs). The numbers of associations are based on number of unique UniProt IDs with at least one significant assay association. The numbers of assay associations are displayed in brackets.

a)		# UniProt ID	# Assay	Age	Sex	BMI
All proteins, Common samples	**SomaScan11K pre-ANML**	9563	10675	445 (486)	1882 (1986)	4361 (4604)
	SomaScan11K ANML	9563	10675	652 (697)	495 (528)	1234 (1304)
	OlinkHT	5401	5405	704	401	1145 (1146)
Common proteins, Common samples	**SomaScan11K pre-ANML**	3718	4424	284 (320)	913 (990)	1621 (1781)
	SomaScan11K ANML	3718	4424	365 (401)	328 (356)	580 (638)
	OlinkHT	3718	3722	629	391	1008 (1009)

b)		# UniProt ID	# Assay	*cis*-pQTLs	*trans*-pQTLs
All proteins, Common samples	**SomaScan11K pre-ANML**	9563	10675	298 (349)	127 (129)
	SomaScan11K ANML	9563	10675	351 (416)	191 (193)
	OlinkHT	5401	5405	300 (305)	16 (17)
Common proteins, Common samples	**SomaScan11K pre-ANML**	3718	4424	186 (219)	37 (38)
	SomaScan11K ANML	3718	4424	218 (262)	59 (60)
	OlinkHT	3718	3722	261 (265)	15 (16)

Figures

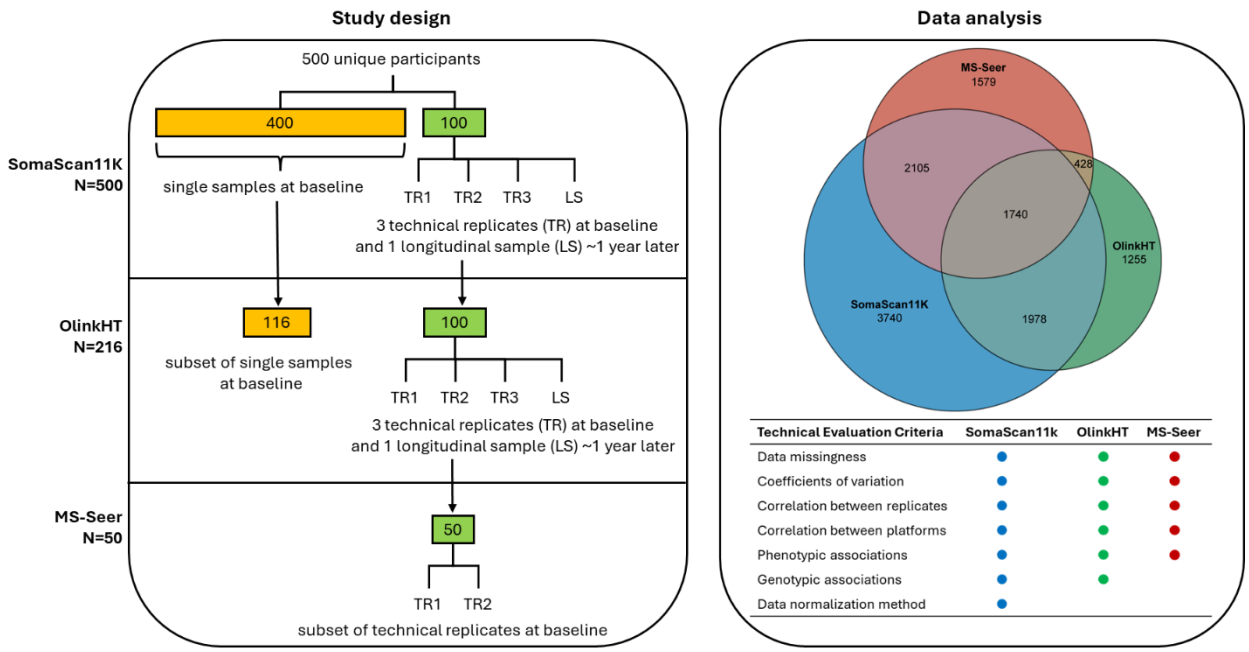

Figure 1. Study design for comparison of plasma proteomic platforms. (Left) Hierarchical sampling workflow of the cohort for the SomaScan11K, OlinkHT, and MS-Seer platforms. (Right, top) Venn diagram depicting the number of proteins uniquely and commonly quantified by three platforms. (Right, bottom) Summary of the seven technical evaluation criteria applied in this study.

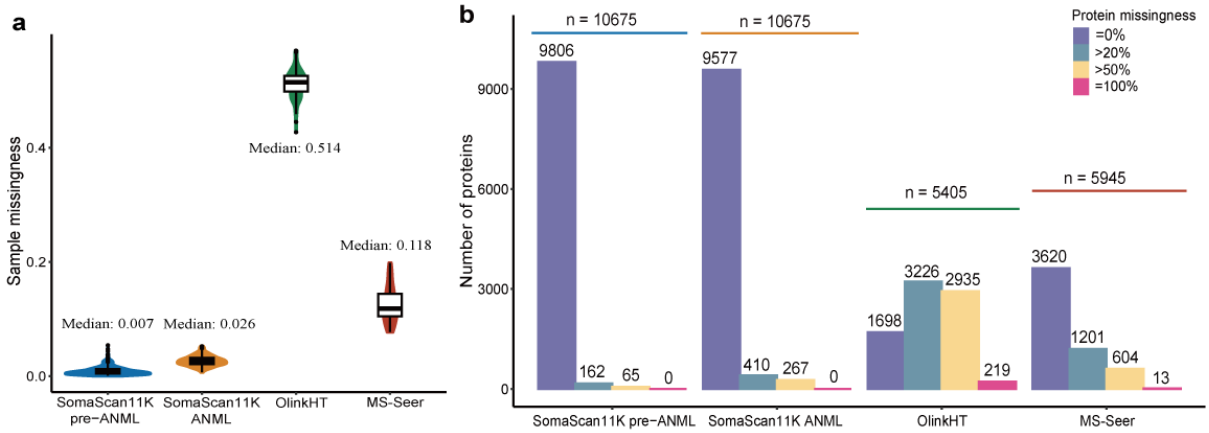

c

CV (%)	Quantile	Intra-plate	Inter-plate
SomaScan11K pre-ANML	0.25	6.98	7.89
	0.50	7.92	9.07
	0.75	9.59	11.43
	0.90	12.39	15.41
SomaScan11K ANML	0.25	3.46	3.97
	0.50	4.61	5.22
	0.75	6.65	7.51
	0.90	9.63	11.48
OlinkHT	0.25	10.30	11.06
	0.50	22.99	23.00
	0.75	109.95	116.12
	0.90	786.17	802.34
MS-Seer	0.25	11.73	
	0.50	18.77	
	0.75	28.76	
	0.90	43.96	

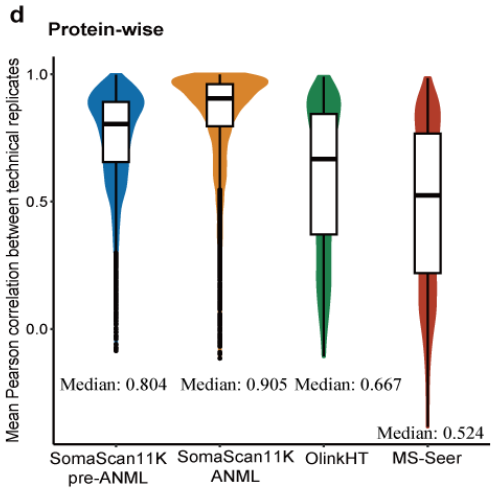

Figure 2. Technical evaluation across SomaScan11K, OlinkHT, and MS-Seer proteomics platforms. (a) Sample-level measurability: violin plots depicting sample missingness for three platforms. (b) Protein-level measurability: bar graph showing the numbers of proteins with different levels of missingness across the platforms, categorized by different thresholds. (c) Precision of measurements: coefficients of variation for SomaScan11K, OlinkHT, and MS-Seer platforms. (d) Technical reproducibility: violin plots showing the mean protein-wise Pearson correlation between technical replicates for three platforms.

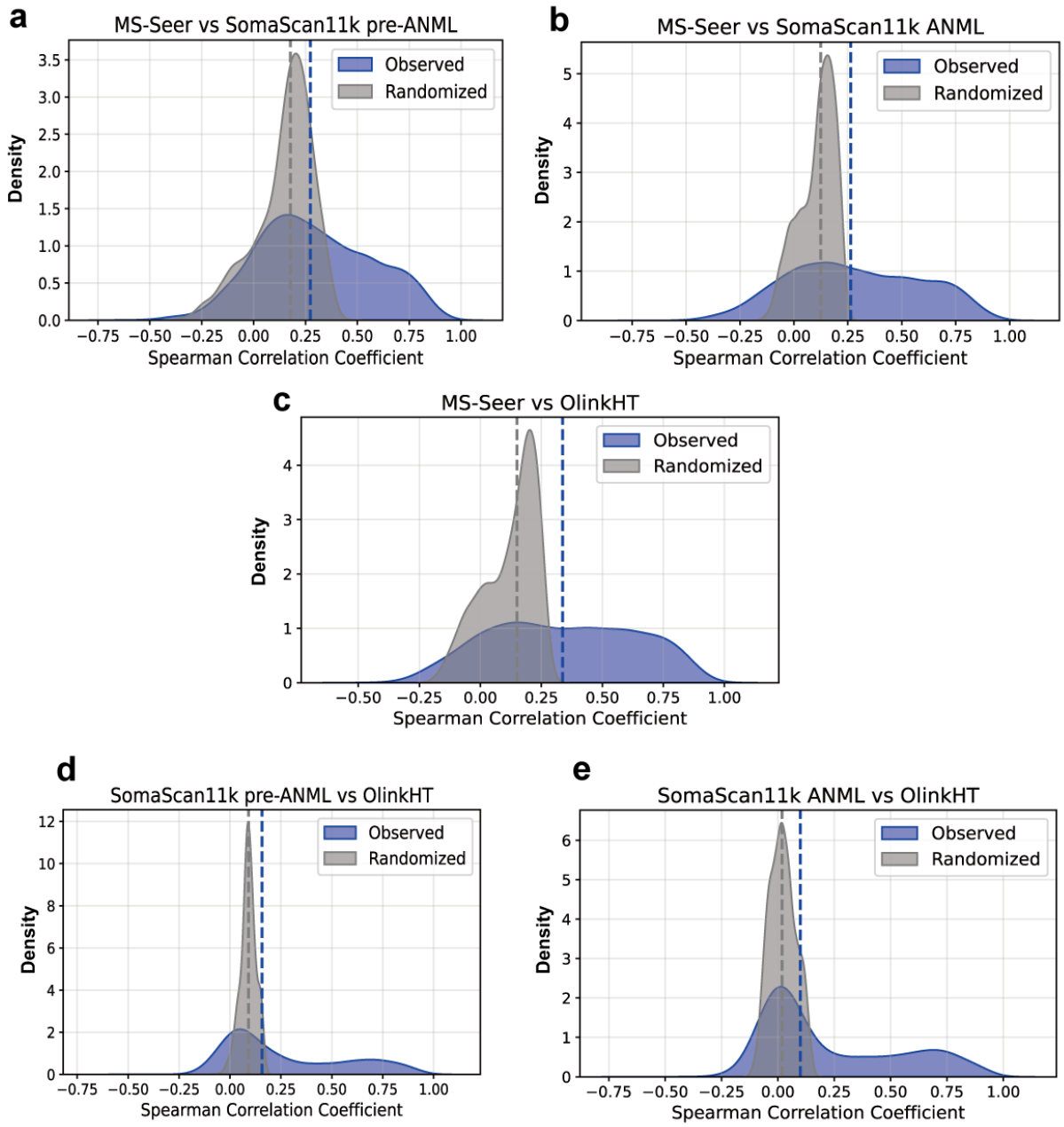

Figure 3. The distribution of protein-wise Spearman correlation between different platform pairs. The distribution in blue is the observed correlation and the grey distribution is the randomized (background) correlation. The blue and grey dotted lines represent the median of each distribution, respectively. (a) Correlation distribution of shared proteins between MS-Seer and SomaScan11K pre-ANML data (b) Correlation distribution of shared proteins between MS-Seer and SomaScan11K ANML data (c) Correlation distribution of shared proteins between MS-Seer and OlinkHT data (d) Correlation distribution of shared proteins between SomaScan11K pre-ANML and OlinkHT data (e) Correlation distribution of shared proteins between SomaScan11K ANML and OlinkHT data.

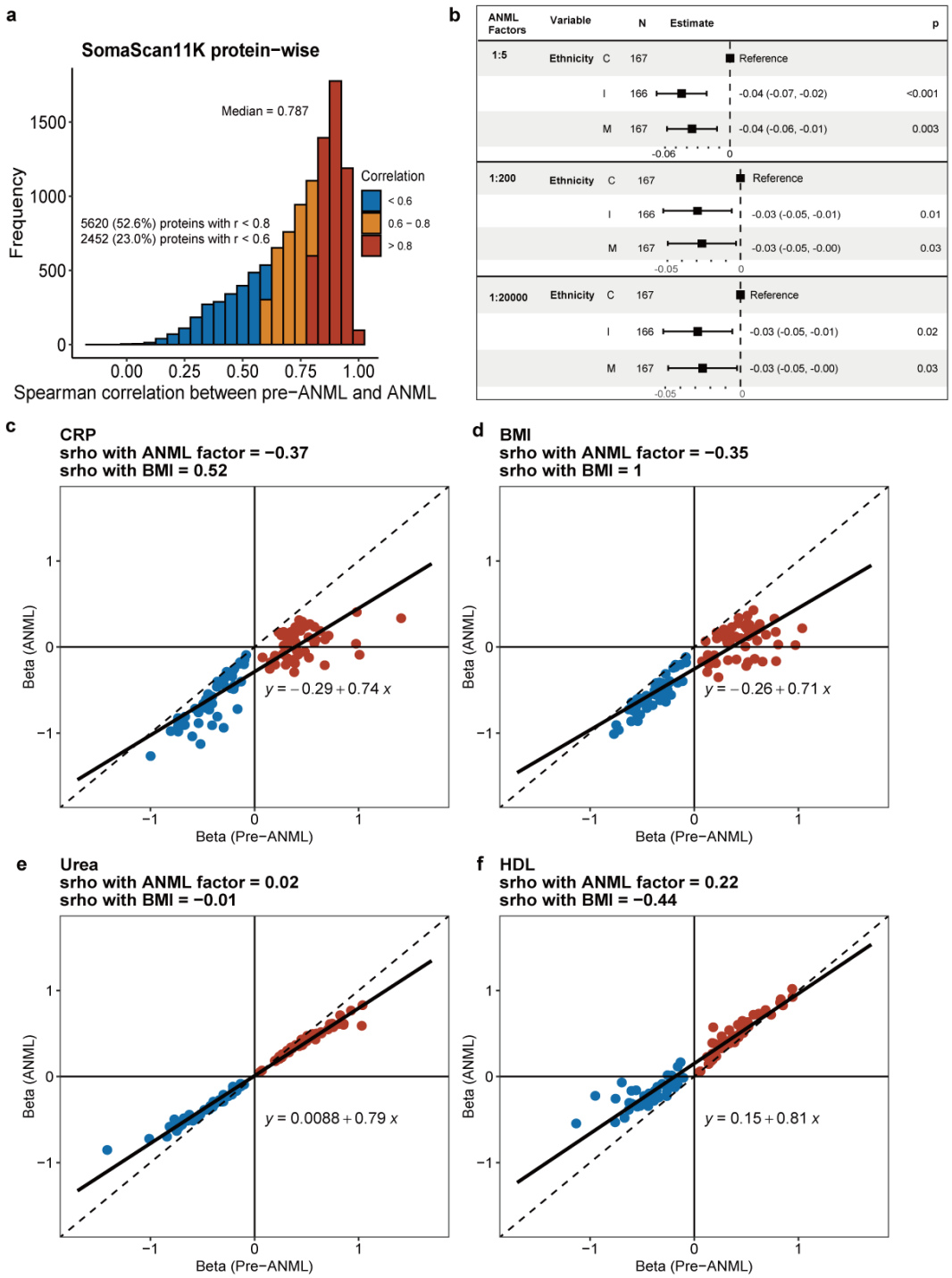

Figure 4. Comparison of SomaScan11K pre-ANML and ANML data. (a) Histogram showing the distribution of protein-wise Spearman correlations between pre-ANML and post-ANML SomaScan11K data. (b) The forests plots depicting the results from fitted linear models (ANML scaling factors ~ ethnicities). (c-f) Effect size comparison for 4 representative phenotypes between pre-ANML and ANML of synthetic proteins generated by simulation method 1: (c) CRP, (d) BMI, (e) Urea and (f) HDL. The Spearman correlations between each phenotype and ANML scaling factor/BMI are shown in each panel title. The dotted and solid lines represent y = x and fitted line, respectively. Red: pre-defined positive effect size; Blue: pre-defined negative effect size.